Fission Dynamics from Scission to Saddle and Beyond

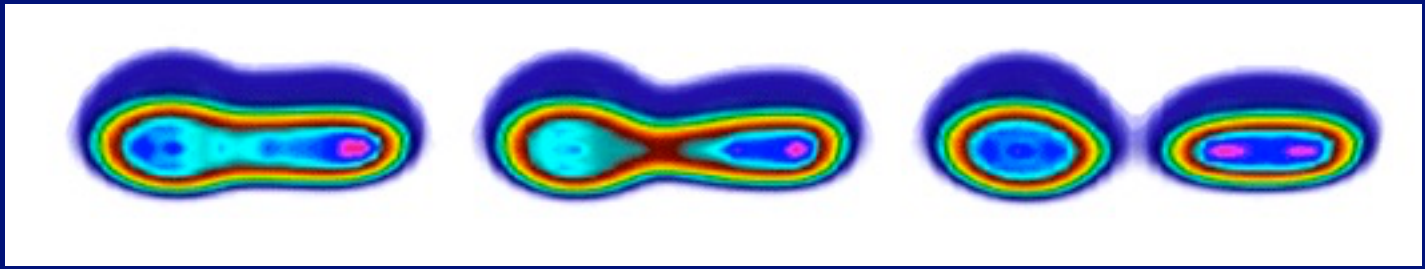

Aurel Bulgac
University of Washington

Collaborators:

Shi Jin ★	**(University od Washington)**
Piotr Magierski	***(Warsaw UT and UoW)***
Kenneth J. Roche ★	**(PNNL and UoW)**
Nicolas Schunck	**(LLNL)**
Ionel Stetcu ★	**(LANL)**

Most of the modeling of fission since 1939 is still performed mostly phenomenologically, *which is distinct from microscopic approaches!*

"Microscopic" approaches (TDGCM, ATDHF) assume the decoupling of collective and intrinsic motion (adiabaticity), making thus the introduction of a collective Hamiltonian legitimate.

Schunck and Robledo, Microscopic theory of nuclear fission, Rep. Prog. Phys. 79, 116301 (2016)
Krappe and Pomorski, Theory of Nuclear Fission, Springer, 2012.

<u>We challenge/disprove this never checked assumption!!!</u>

What <u>microscopic</u> conclusions have been firmly established so far?

- **Fission is controlled by the competition between Coulomb and surface energies.** ***Meitner and Frisch (1939)***

- **The formation of a compound nucleus and a very slow evolution of the nuclear shape towards the outer barrier.** ***Bohr and Wheeler*** **(1939)**

- **The crucial role of shell effects at large deformations and of the pairing correlations while the nuclear shape evolves.** ***Strutinski, 1967, Bertsch, 1980***

- **The decay of the fission fragments can be described in a statistical approach.** ***Weisskopf (1937), Hauser and Feshbach (1952)***

The Main Theoretical Tool

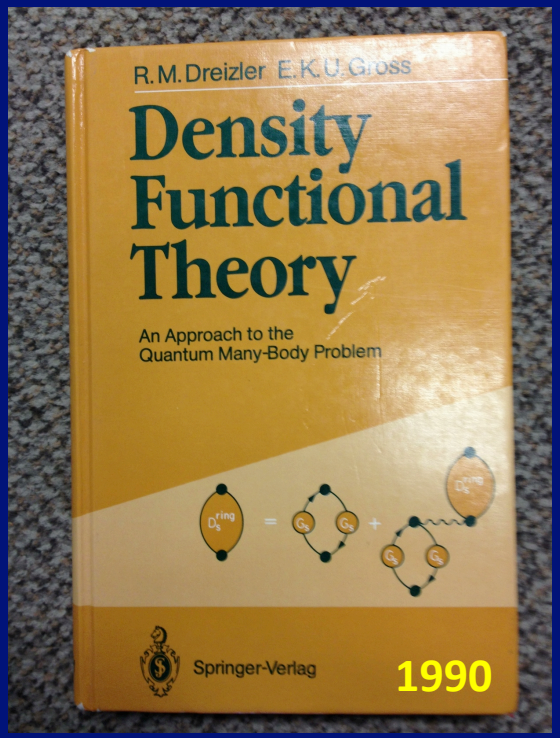

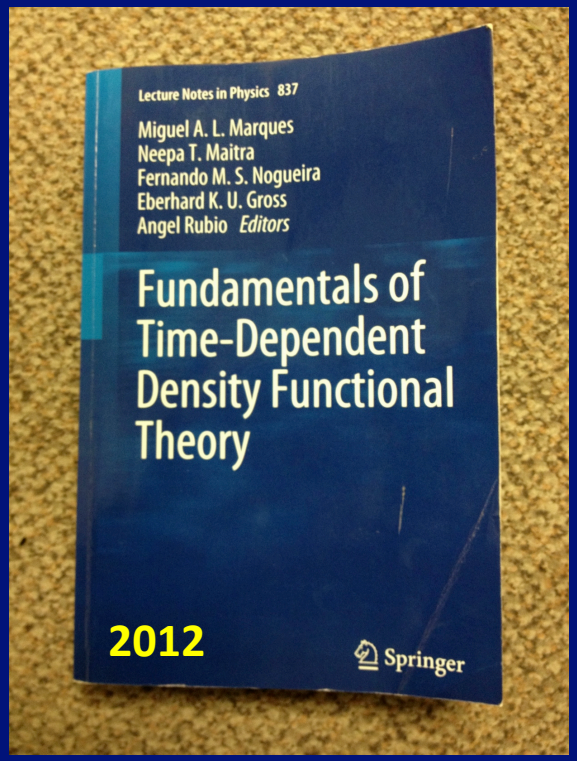

DFT has been developed and used mainly to describe normal (non-superfluid) electron systems – more than 50 years old theory, Kohn and Hohenberg, 1964

A new local extension of DFT to superfluid systems and time-dependent phenomena was developed

Review: A. Bulgac, *Time-Dependent Density Functional Theory and Real-Time Dynamics of Fermi Superfluids*, Ann. Rev. Nucl. Part. Sci. 63, 97 (2013)

The Main Computational Tool

Cray XK7, ranked at peak ≈ 27 Petaflops (Peta – 10^{15})
On Titan there are 18,688 GPUs which provide 24.48 Petaflops !!!
and 299,008 CPUs which provide only 2.94 Petaflops.

A single GPU using a CUDA code on Titan performs the same amount of FLOPs as approximately 150 CPUs using a C code. Piz Daint is about 3x faster, and Summit 1,4x faster than Piz Daint
Jaguar, Titan, Piz Daint, Tsubame 3.0, and Summit in the future

The Main Theoretical Tool: DFT

TDSLDA- This is an extension to Superfluids and Time-Dependent Phenomena of DFT and is based on Verification and Validation for a variety of strongly interacting fermions systems (cold atoms, neutron star crust, nuclei).

- **Since DFT/SLDA is not an approximation, but in principle an exact theoretical framework (unlike HF, HFB, etc.), one has to convincingly prove that its specific realization is equivalent to the Schrödinger equation!**
- **(*The fine print: There is a continuous debate on whether DFT exist for self-bound systems, but this will not be discussed today. If you feel more confortable for the sake of the discussion replace DFT with EDF. . In the distant future one might be create traps for nuclei, using x-and gamma lasers, as they do for cold atoms)***
- **<u>The DFT and the Schrödinger descriptions of observables should be identical.</u>**
- **One expects that DFT also describes correctly Nature!**
- **And, of course, that the numerical implementation faithfully reproduces the theory.**

$$i\hbar\frac{\partial}{\partial t}\begin{pmatrix} u_{n\uparrow}(\vec{r},t) \\ u_{n\downarrow}(\vec{r},t) \\ v_{n\uparrow}(\vec{r},t) \\ v_{n\downarrow}(\vec{r},t) \end{pmatrix} = \begin{pmatrix} \hat{h}_{\uparrow\uparrow}(\vec{r},t)-\mu & \hat{h}_{\uparrow\downarrow}(\vec{r},t) & 0 & \Delta(\vec{r},t) \\ \hat{h}_{\downarrow\uparrow}(\vec{r},t) & \hat{h}_{\downarrow\downarrow}(\vec{r},t)-\mu & -\Delta(\vec{r},t) & 0 \\ 0 & -\Delta^{*}(\vec{r},t) & -\hat{h}^{*}_{\uparrow\uparrow}(\vec{r},t)+\mu & -\hat{h}^{*}_{\uparrow\downarrow}(\vec{r},t) \\ \Delta^{*}(\vec{r},t) & 0 & -\hat{h}^{*}_{\downarrow\uparrow}(\vec{r},t) & -\hat{h}^{*}_{\downarrow\downarrow}(\vec{r},t)+\mu \end{pmatrix} \begin{pmatrix} u_{n\uparrow}(\vec{r},t) \\ u_{n\downarrow}(\vec{r},t) \\ v_{n\uparrow}(\vec{r},t) \\ v_{n\downarrow}(\vec{r},t) \end{pmatrix}$$

How important is pairing?

Without pairing nuclei will typically will not fission!!!

^{240}Pu fission in the normal pairing gap

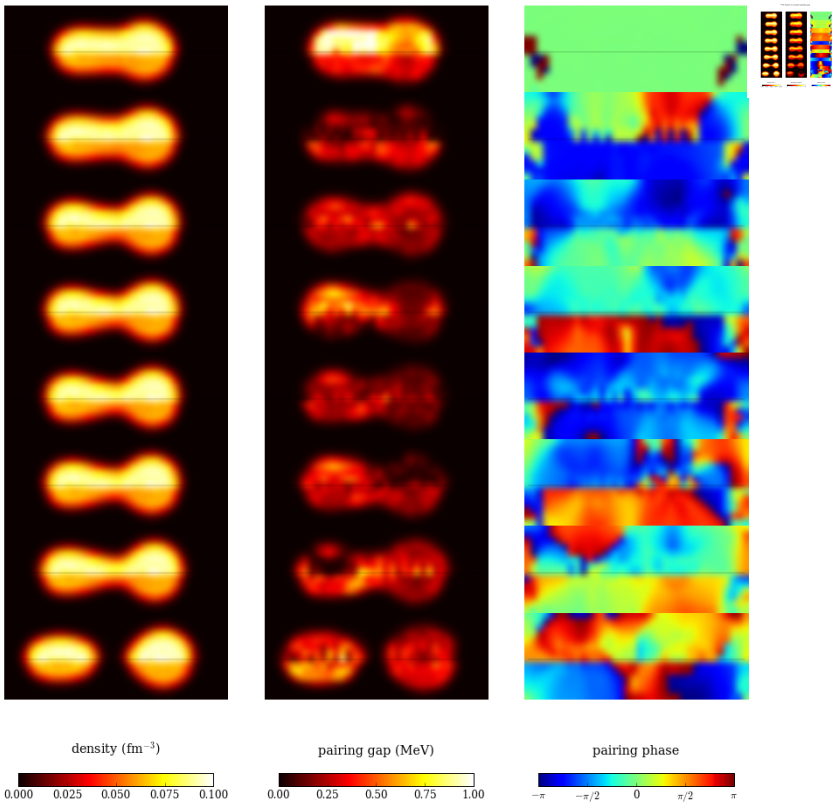

^{240}Pu fission in a larger pairing gap

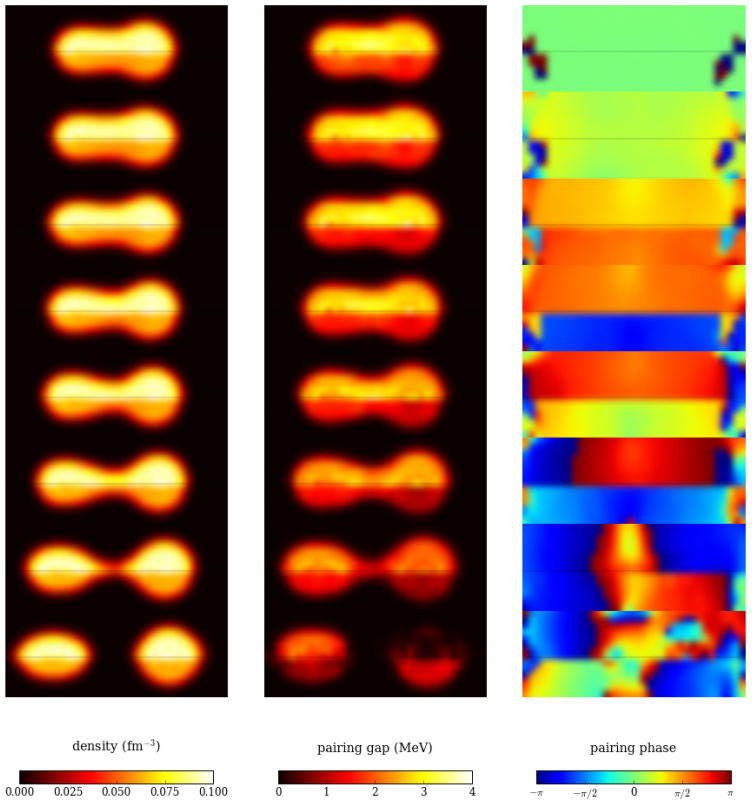

Normal pairing strength
Saddle-to-scission 14,000 fm/c

Enhanced pairing strength
Saddle-to-scission 1,400 fm/c !!!

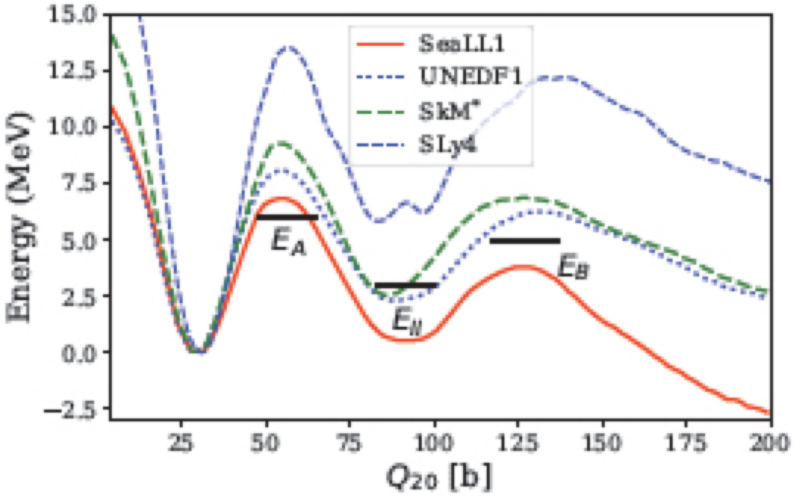
SeaLL1
UNEDF1
SkM*
SLy4
E_A
E_B
E_{II}
Energy (MeV)
Q_{20} [b]

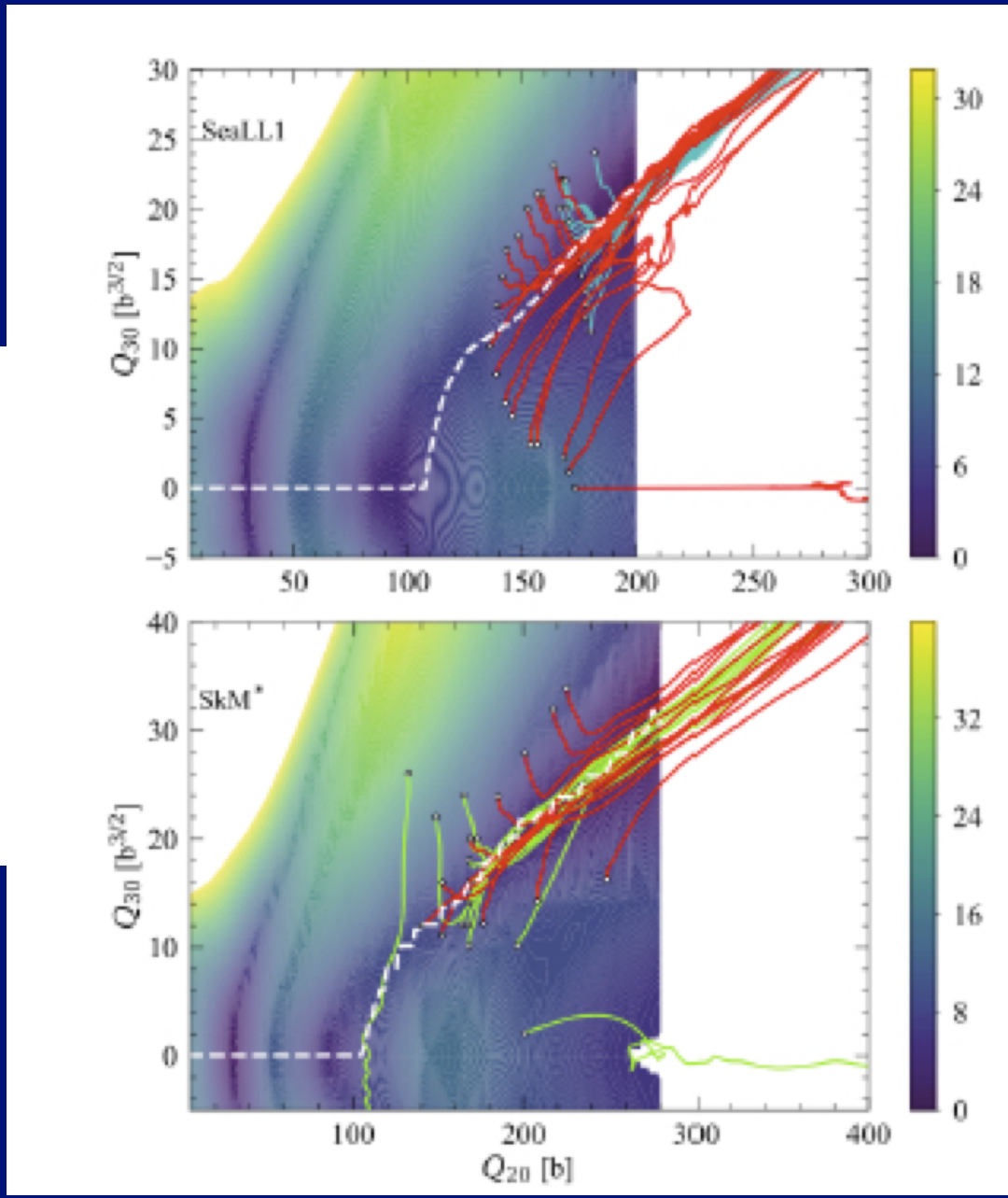
SeaLL1
SkM*
Q_{30} [b$^{3/2}$]
Q_{20} [b]

NEDF	$E^*_{\rm ini}$	TKE	$N_{\rm H}$	$Z_{\rm H}$	$N_{\rm L}$	$Z_{\rm L}$	$E^*_{\rm H}$	$E^*_{\rm L}$	TXE	TKE+TXE	$\tau_{s\to s}$ (fm/c)
SeaLL1-1asy	7.9(1.7)	177.8(3.1)	83.4(0.4)	53.2(0.4)	62.9(0.5)	41.1(0.4)	17.1(3.0)	20.3(2.0)	37.4(3.1)	215.2(2.5)	2317(781)
SeaLL1-2asy	2.6(1.8)	178.0(2.3)	82.9(0.4)	52.9(0.2)	63.3(0.5)	41.5(0.3)	19.5(3.8)	14.0(1.9)	33.5(5.1)	211.5(3.3)	1460(176)
SeaLL1-sy	9.2	147.1	77.5	48.9	68.8	45.4	45.2	29.0	74.2	221.3	10103
SkM*-1asy	8.2(3.0)	174.5(2.5)	84.1(0.9)	53.0(0.5)	61.8(0.9)	40.9(0.5)	16.6(3.1)	14.9(2.3)	31.5(3.8)	206.0(2.4)	1214(448)
SkM*-1sy	9.6	149.0	73.4	47.2	72.6	46.7	29.4	28.5	57.9	206.9	3673
SkM*-2asy	8.1(0.2)	182.8(4.4)	82.6(1.0)	52.4(0.6)	63.6(1.0)	41.7(0.5)	14.3(3.9)	13.0(3.0)	27.3(3.4)	210.1(1.8)	1349(309)

Table I. The NEDF, the initial excitation energy $E^*_{\rm ini}$, TKE, neutron, proton number, and excitation energies of the heavy and light fragments, total excitation energy of fragments TXE, and the sum of TKE and TXE, and the average saddle-to-scission times and their corresponding variances in parentheses. All energies are in MeV and S***sy, S***asy stand for symmetric and antisymmetric channels. Using Wahl's charge systematics [89] and data from Ref. [90] one obtains for neutrons $N_L^{syst} \approx 61$ and $N_H^{syst} \approx 85$ and for protons $Z_L^{syst} \approx 40$ and $Z_H^{syst} \approx 54$, and $\mathrm{TKE}^{syst} = 177 \ldots 178$ MeV from Ref. [91].

NEDF	$T_{\rm L}$ [MeV]	$T_{\rm H}$ [MeV]	$T_{\rm L}$ [MeV]	$T_{\rm H}$ [MeV]	$Q^{\rm L}_{20}$ [b]	$Q^{\rm H}_{20}$ [b]	$Q^{\rm L}_{30}$ [b$^{3/2}$]	$Q^{\rm H}_{30}$ [b$^{3/2}$]	$(c/a)_H$	$(c/a)_L$	$\tau_{s\to s}$ [fm/c]
SeaLL1-1	1.40(0.07)	1.11(0.08)	1.28(0.07)	1.16(0.07)	15.7(0.9)	2.6(0.5)	0.08(0.17)	–0.20(0.06)	1.06(0.01)	1.59(0.03)	2392(800)
SeaLL1-2	1.15(0.08)	1.19(0.12)	1.00(0.08)	1.21(0.08)	17.1(1.1)	2.6(0.6)	0.23(0.08)	–0.19(0.06)	1.06(0.01)	1.63(0.03)	1460(176)
SeaLL1-sy	1.54	1.99			27.4	27.0	0.9	-1.1	1.87	1.73	10103
SkM*-1asy	1.20(0.09)	1.10(0.10)			11.3(1.3)	3.5(0.9)	0.1(0.1)	–0.4(0.1)	1.08(0.02)	1.42(0.04)	1214(448)
SkM*-1sy	1.56	1.55			24.2	25.6	0.9	-1.0	1.72	1.75	3673
SkM*-2asy	1.11(0.14)	1.02(0.14)			14.5(1.7)	2.3(0.7)	0.09(0.08)	–0.3(0.1)	1.05(0.02)	1.53(0.06)	1349(309)

Table II. Internal temperatures for the light $T_{\rm L}$ and heavy $T_{\rm H}$ fragments computed according to the simple estimate (columns 2 and 3) or finite-temperature HFB calculations (columns 4 and 5). The axial quadrupole and octupole moments of the fragments, the ratios of the long to the short semi-axes, as well as the average scission times are also listed

Scission

Heavy fission fragment

Light fission fragment

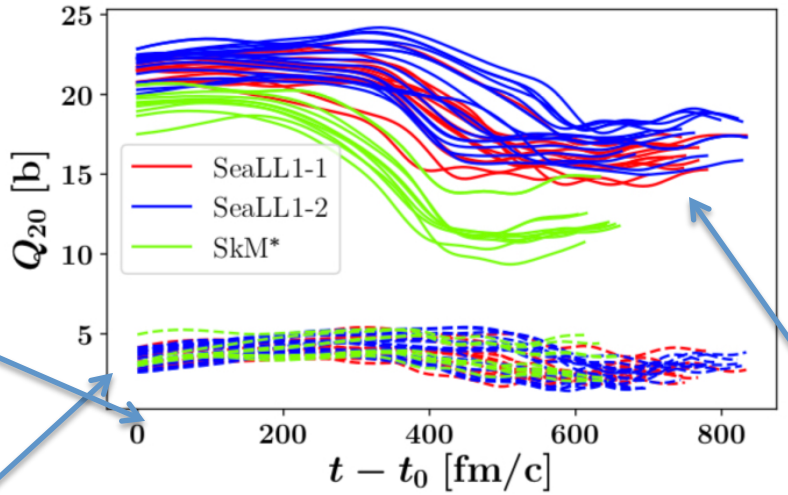

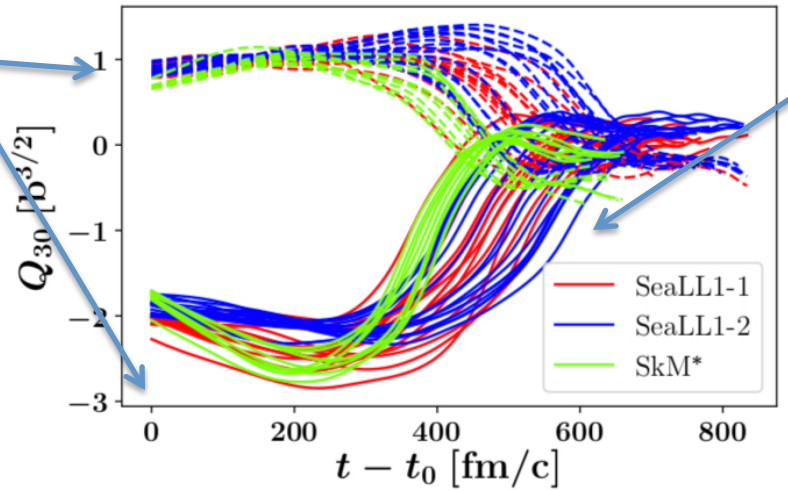

Figure 5. (Color online) The evolution of the quadrupole Q_{20} and octupole Q_{30} moments of the light (solid lines) and heavy (dashed lines) FFs after scission. The color codes are the same as in Fig. 3

The light fission fragment emerges at scission (t_0) very elongated, but it relaxes relatively quickly.

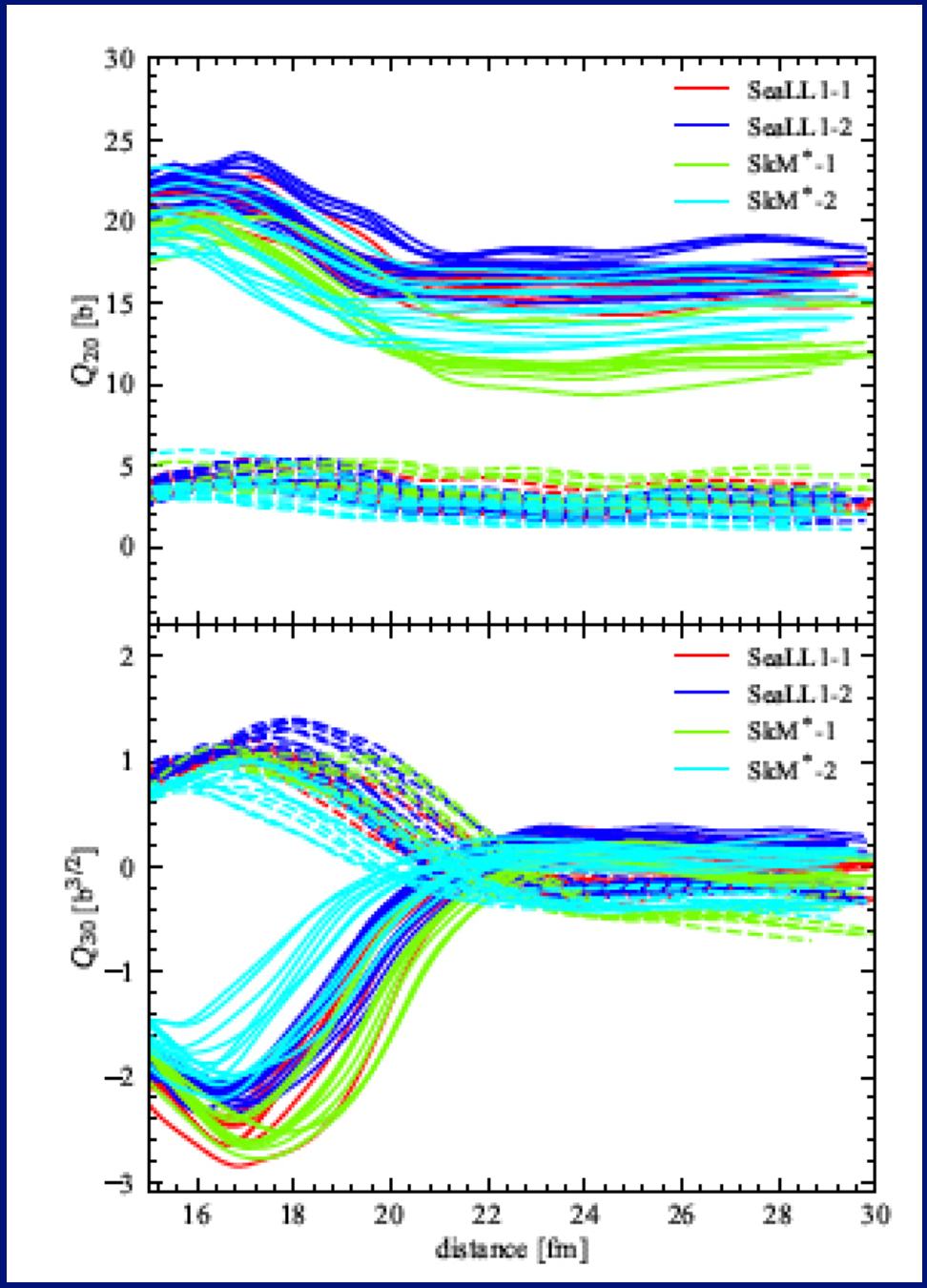
SeaLL1-1
SeaLL1-2
SkM*-1
SkM*-2
Q_{20} [b]
Q_{30} [b$^{3/2}$]
distance [fm]

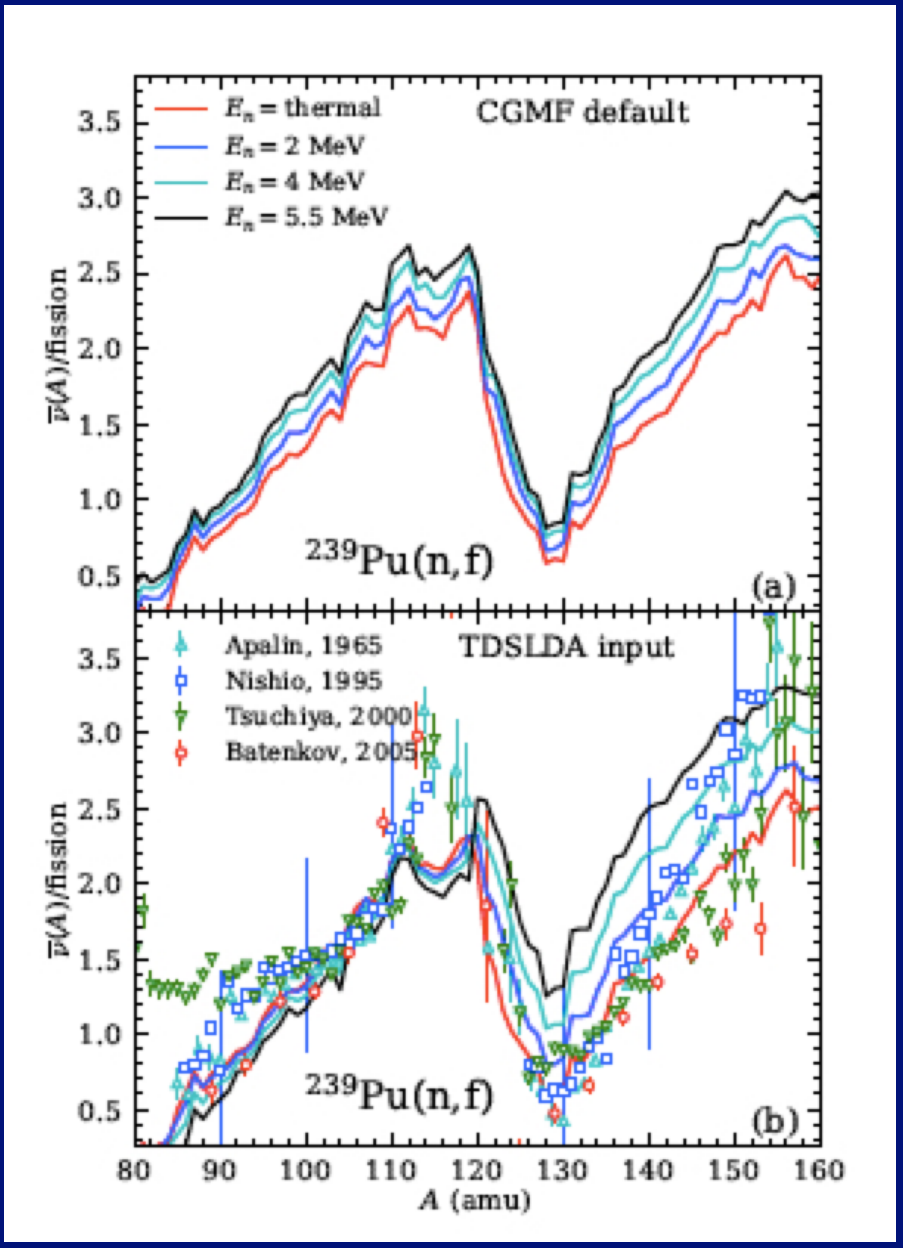

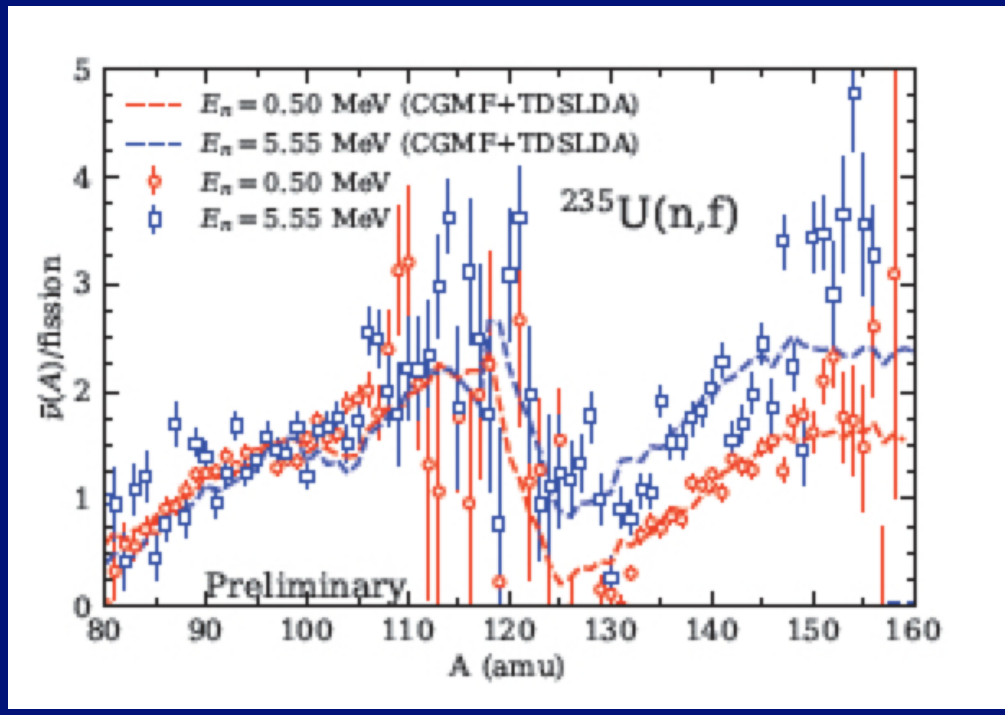

TDSLDA, unlike other approaches, predicts the excitation energy sharing between FFs.

Large Amplitude Collective Motion is strongly dissipative. It is overdamped! It is slower than adiabatic motion!!!

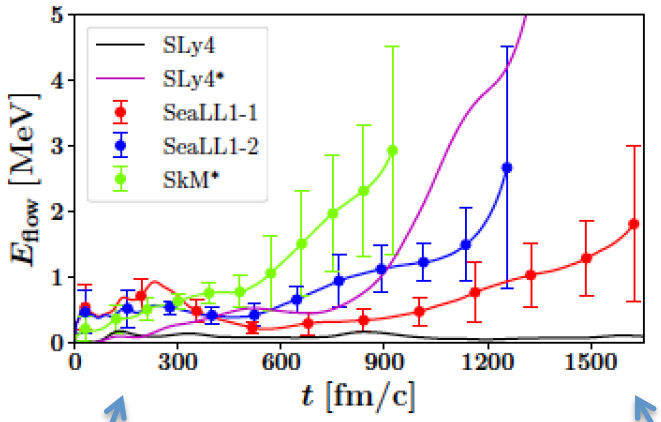

Figure 3. (Color online) The collective flow energy evaluated for NEDFs with realistic pairing SLy4 [41], enhanced pairing SLy4*, and for SkM*, SeaLL1-1 and SeaLL1-2 sets. The error bars illustrate the size of the variations due to different initial conditions.

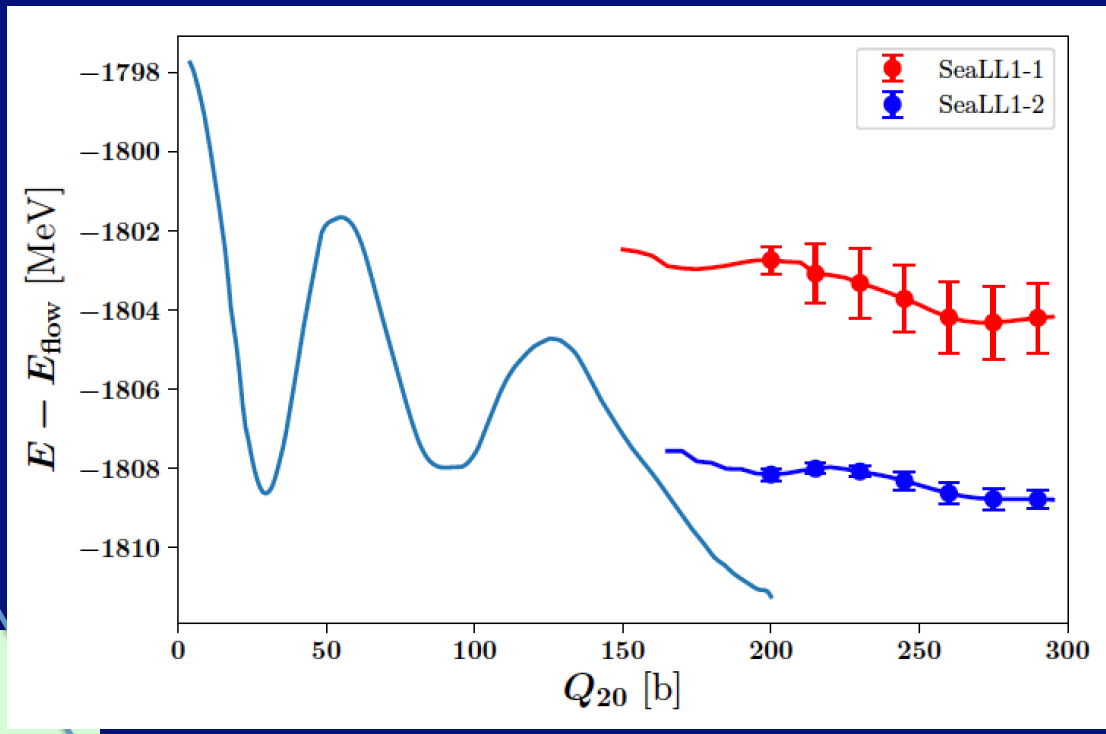

$$E_{flow} = \int d^3r \frac{\vec{j}^2(\vec{r},t)}{2mn(\vec{r},t)}$$

$$\vec{j}(\vec{r},t) = \frac{i\hbar}{2}\sum_k \mathrm{v}_k^*(\vec{r},t)\vec{\nabla}\mathrm{v}_k(\vec{r},t) - \mathrm{v}_k(\vec{r},t)\vec{\nabla}\mathrm{v}_k^*(\vec{r},t)$$

$$n(\vec{r},t) = \sum_k \left|\mathrm{v}_k(\vec{r},t)\right|^2$$

$$E_{total} = E_{flow} + E_{\rm int} \approx E_{\rm int}(q,T) \approx const.$$

$$E_{\rm int} = V(q,T) \approx const$$

The kinetic energy of the fission fragments at scission is almost negligible, an order of magnitude smaller then expected in all "microscopic" models!

Fission Fragments emerge (relatively) "hot" at scission!

And they will get a bit hotter after their shape relaxes, particularly the light fragments.

A little gedanken experiment!

The energy flow from the collective degrees of freedom to intrinsic degrees of freedom is irreversible!

The entropy and the temperature of the intrinsic system are increasing while the nucleus evolves towards the scission configuration.

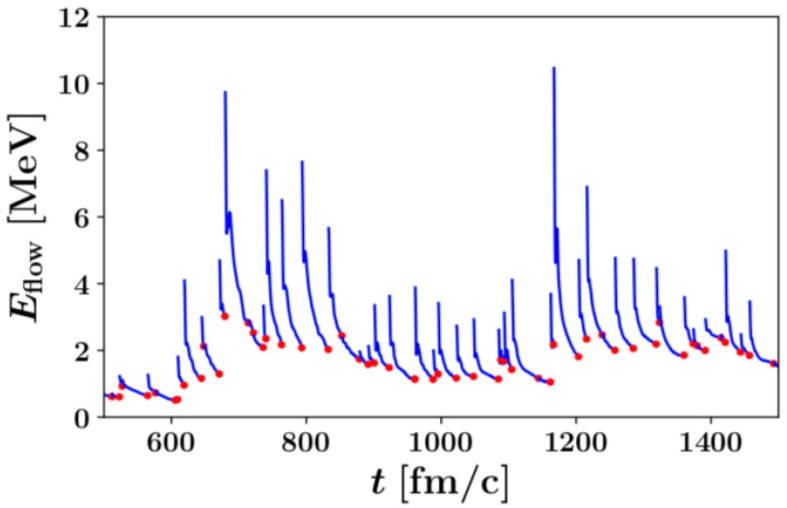

Figure 3. (Color online) At times indicated with red dots we have applied collective quadrupole momentum kicks to both neutrons and protons, see Eq. (15), with random values of η, see Eq. (15).

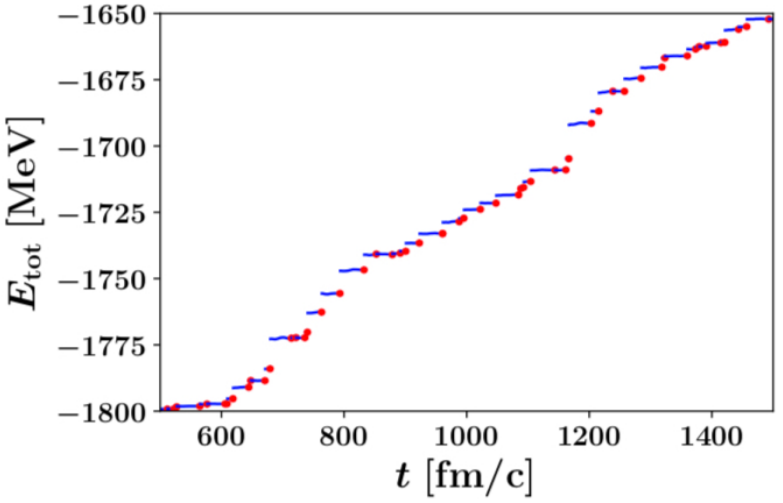

Figure 4. The time evolution of the total energy of the nucleus, in the rest frame of the nucleus, after we have applied collective kicks were to both neutrons and protons with random values of η, see Eq. (15) and Fig. 3.

$$\begin{pmatrix} u_\alpha(\mathbf{r},t) \\ v_\alpha(\mathbf{r},t) \end{pmatrix} \rightarrow \begin{pmatrix} \exp[\, i\eta(2z^2 - x^2 - y^2)]u_\alpha(\mathbf{r},t) \\ \exp[-i\eta(2z^2 - x^2 - y^2)]v_\alpha(\mathbf{r},t) \end{pmatrix}$$

$$E_{tot} = E_{flow} + E_{\rm int} \approx E_{\rm int}$$

- **The irreversible energy flow from the collective degrees of freedom towards the intrinsic degrees of freedom is simply controlled by the large entropy of the intrinsic system.**
  At the scission configuration the level density is about 10^7 MeV^{-1}.

$$S_{tot}(t) = -\mathrm{Tr}_{all}\ \rho_{tot}(t)\ln\rho_{tot}(t) \equiv 0, \quad \rho_{tot}(t) = \left|\Psi(t)\right\rangle\left\langle\Psi(t)\right|,$$
$$S_{\mathrm{int}}(t) = -\mathrm{Tr}_{\mathrm{int}}\ \rho_{\mathrm{int}}(t)\ln\rho_{\mathrm{int}}(t) \quad \geq 0 \Leftarrow \text{Entanglement entropy},$$
$$\rho_{\mathrm{int}}(t) = \mathrm{Tr}_{coll}\ \rho_{tot}(t)$$

Intrinsic entropy is the main driver of the nuclear shape dynamics

Does there exist a GCM/ATDHF-like representation of the total nuclear wave function?

$$\left|\Psi\right\rangle = \int d^n q f(q_1,\ldots,q_n)\left|q_1,\ldots,q_n\right\rangle$$

$N_s = 24^2 \times 48 = 27{,}648$ sites on spatial lattice in a typical simulation

the maximum number of collective coordinates

$$N_{\mathrm{SD}} = \frac{(2N_s)!}{Z!(2N_s - Z)!} \times \frac{(2N_s)!}{N!(2N_s - N)!} \simeq 10^{739} \quad \#\text{ of possible Slater det.}$$

<u>The fine print!</u>

Nobody produced yet a theoretical argument which determines how many and what kind of collective degrees of freedom are necessary!

Very likely their number Increases while a nucleus barrels down from near the saddle all the way to scission.

- **Not an exact numerical estimate for N_s, but a reasonable one.**
- **A satisfactory physical framework would require about 10^7 Slater determinants at scission.**

What have we learned?

Large Amplitude Collective Motion is strongly dissipative, it is overdamped, the role of the collective inertia is negligible!

The introduction of a collective Hamiltonian is illegitimate.

Fluctuations or two-body collisions do not modify this conclusion.

What is the relevance of this finding for our understanding and description of fission dynamics?

Including dissipation and fluctuations

Classically, Langevin equation:

$$m\ddot{x}(t) = F - \gamma m\dot{x}(t) + m\xi(t),$$

$$\langle \xi(t) \rangle = 0, \quad \langle \xi(t)\xi(t') \rangle = \Gamma\delta(t-t'),$$

$$\dot{x}(t) = \mathrm{v}(0)\exp(-\gamma t) + \frac{F}{m\gamma}\left(1-\exp(-\gamma t)\right) + \int_0^t dt'\xi(t)\exp(-\gamma(t-t')),$$

$$\langle \mathrm{v}(t) \rangle \to \frac{F}{m\gamma}, \quad \langle\langle \mathrm{v}^2(t) \rangle\rangle \to \frac{\Gamma}{2\gamma} = \frac{T}{m}$$

Quantum mechanically, Lindblad equation:

$$i\hbar\dot{\rho} = \left[H, \rho\right] - i\left(W\rho + \rho W\right) + i\sum_{k,l} h_{kl} A_k \rho A_l^\dagger,$$

$$W = W^\dagger = \frac{1}{2}\sum_{k,l} h_{kl} A_l^\dagger A_k, \quad h_{kl} = h_{lk}^*, \quad \mathrm{Tr}\dot{\rho} = 0.$$

A much better and simpler solution:
A quantum Hermitian "Langevin" equation

Quantum friction

$$i\hbar\dot{\psi}_k(\vec{r},t) = h\Big[n(\vec{r},t)\Big]\psi_k(\vec{r},t) + \gamma\Big[n(\vec{r},t)\Big]\dot{n}(\vec{r},t)\psi_k(\vec{r},t)$$
$$-\frac{1}{2}\Big[\vec{u}(\vec{r},t)\cdot\vec{p} + \vec{p}\cdot\vec{u}(\vec{r},t)\Big]\psi_k(\vec{r},t) + \varsigma(\vec{r},t)\psi_k(\vec{r},t)$$

"Stochastic fields"

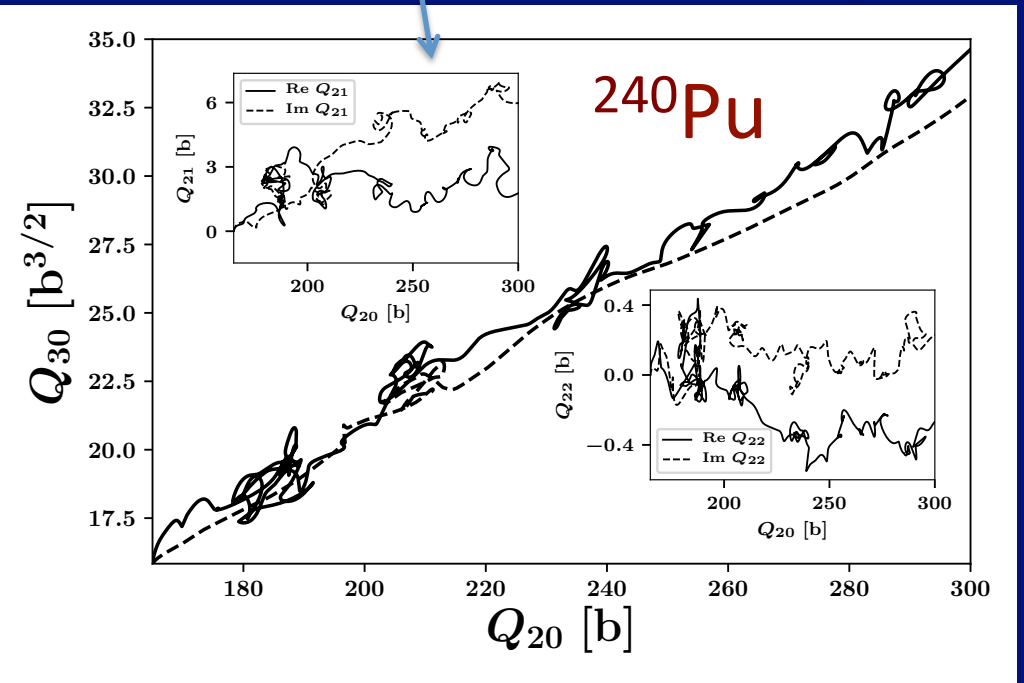

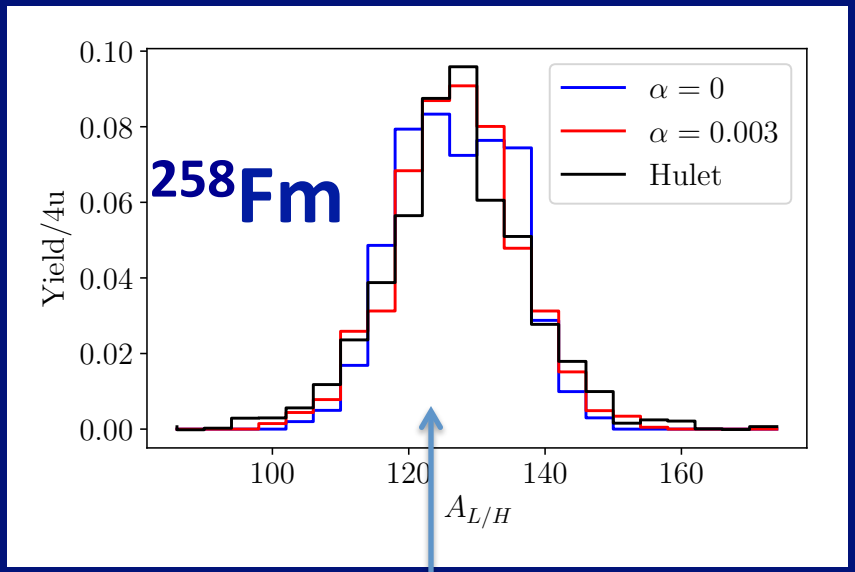

Mass yields
Without shell corrections

Summary

- **While pairing is not the engine driving the fission dynamics, pairing provides the essential lubricant, without which the evolution may arrive quickly to a screeching halt.**

- **TDDFT will offer insights into nuclear processes and quantities which are either not easy or impossible to obtain in the laboratory: fission fragments excitation energies and angular momenta distributions prior to neutron and γ emission, element formation in astrophysical environments, and other nuclear reactions in a parameter free approach …**

- **The quality of the agreement with experimental observations is surprisingly good, especially taking into account the fact that we made no effort to reproduce any fission measured data. No fitting of parameters!**

- **It has been now firmly established microscopically that large amplitude collective motion is strongly dissipative and overdamped and phenomenological models would have to be altered accordingly.**

- **The fissioning nucleus behaves superficially as a very viscous system.**

- **The "temperatures" of the fission fragments are not equal.**

A new promising NEDF: SeaLL1

- ✓ This un-optimized NEDF SeaLL1 is physically intuitive and at the present level provides one of the most accurate descriptions of global nuclear properties (masses, charge radii, two-nucleon separation energies, single-particle spectra, etc.) with a surprisingly small number of parameters (seven).
- ✓ The outlined framework provides a clear strategy for further improving the quality of NEDF.
- ✓ Equation of State of Infinite Neutron Matter properties inferred from QCM included.
- ✓ We have identified a significant number of parameters, which have little or no influence on the ground state properties. These additional parameters can be used to refine various nuclear properties, basically without affecting masses and radii.

  - Single-particle spectra
  - Static dipole polarizability
  - Neutron skin thickness
  - Symmetry energy properties
  - Isovector giant resonance properties
  - Gamow-Teller and beta transitions
  - Nuclear compressibility and monopole giant resonances
  - Pairing properties

The full form of the functional SeaLL1 is

$$\mathcal{E}[n_n,n_p] = \overbrace{\frac{\hbar^2}{2m}(\tau_n+\tau_p)}^{\text{kinetic}} + \overbrace{\sum_{j=0}^{2}(a_j n^{5/3} + b_j n^2 + c_j n^{7/3})\beta^{2j}}^{\text{homogeneous}} + \overbrace{\eta_s \sum_{q=n,p}\frac{\hbar^2}{2m}|\nabla n_q|^2}^{\text{gradient}}$$

$$+ \underbrace{W_0 \boldsymbol{J}\cdot\nabla n}_{\text{spin-orbit}} + \underbrace{\sum_{q=n,p} g_{\text{eff}}(\boldsymbol{r})|v_q(\boldsymbol{r})|^2}_{\text{pairing}} + \underbrace{\frac{e^2}{2}\int d^3\boldsymbol{r}'\frac{n_p(\boldsymbol{r})n_p(\boldsymbol{r}')}{|\boldsymbol{r}-\boldsymbol{r}'|} - \frac{e^2\pi}{4}\left[\frac{3n_p(\boldsymbol{r})}{\pi}\right]^{4/3}}_{\text{Coulomb}}.$$

- ✓ **Terms not previously considered in literature proportional to $n^{5/3}$ and no higher powers higher than $n^{7/3}$!**
- ✓ **The apparent number of 9 (a,b,c's) + η_s+W_0+g_0 (volume pairing) = 12 parameters eventually comes down to only seven parameters!**

$$n(\boldsymbol{r}) = \sum_{k,\sigma} v^*_{k\sigma}(\boldsymbol{r})v_{k\sigma}(\boldsymbol{r}), \qquad n = n_n + n_p, \qquad \beta = \frac{n_n - n_p}{n_n + n_p},$$

$$\nu(\boldsymbol{r}) = \sum_{k} v^*_{k\uparrow}(\boldsymbol{r})u_{k\downarrow}(\boldsymbol{r}),$$

$$\tau(\boldsymbol{r}) = \sum_{k,\sigma} \nabla v^*_{k\sigma}(\boldsymbol{r})\cdot\nabla v_{k\sigma}(\boldsymbol{r}),$$

$$\boldsymbol{J}(\boldsymbol{r}) = \frac{\nabla-\nabla'}{2\mathrm{i}}\times\sum_{k,\sigma,\sigma'} v^*_{k\sigma}(\boldsymbol{r})\sigma_{\sigma,\sigma'}v_{k\sigma'}(\boldsymbol{r}')\Big|_{\boldsymbol{r}=\boldsymbol{r}'},$$

Time-even densities

$$s(\boldsymbol{r}) = \sum_{k,\sigma,\sigma'} v^*_{k\sigma}(\boldsymbol{r})\sigma_{\sigma,\sigma'}v_{k\sigma'}(\boldsymbol{r}),$$

$$\boldsymbol{j}(\boldsymbol{r}) = \sum_{k,\sigma}\frac{\nabla-\nabla'}{2\mathrm{i}}v^*_{k\sigma}(\boldsymbol{r}')v_{k\sigma}(\boldsymbol{r})\Big|_{\boldsymbol{r}=\boldsymbol{r}'};$$

Time-odd densities

QMC EOS of infinite homogeneous neutron matter

(allows us to fix three parameters)

$$\mathcal{E}(n_n,n_p) = \frac{3\hbar^2(3\pi^2)^{2/3}}{10m}\left(n_n^{5/3}+n_p^{5/3}\right) + \sum_{j=0}^{2}(a_j n^{5/3} + b_j n^2 + c_j n^{7/3})\beta^{2j}.$$

$$\mathcal{E}_n(n_n) = \frac{3\hbar^2}{10m_n}(3\pi^2 n_n)^{2/3} n_n + \mathcal{E}_{\rm int}(n_n),$$

$$\mathcal{E}_{\rm int}(n_n) = a_n n_n^{5/3} + b_n n_n^2 + c_n n_n^{7/3},$$

Values fixed from QMC with chiral EFT 2N (N3LO) and 3N (N2LO) interactions

$$a_n = a_0 + a_1 + a_2 = -32.6\,\text{MeV fm}^2,$$

$$b_n = b_0 + b_1 + b_2 = -115.4\,\text{MeV fm}^3,$$

$$c_n = c_0 + c_1 + c_2 = 109.1\text{MeV fm}^4.$$

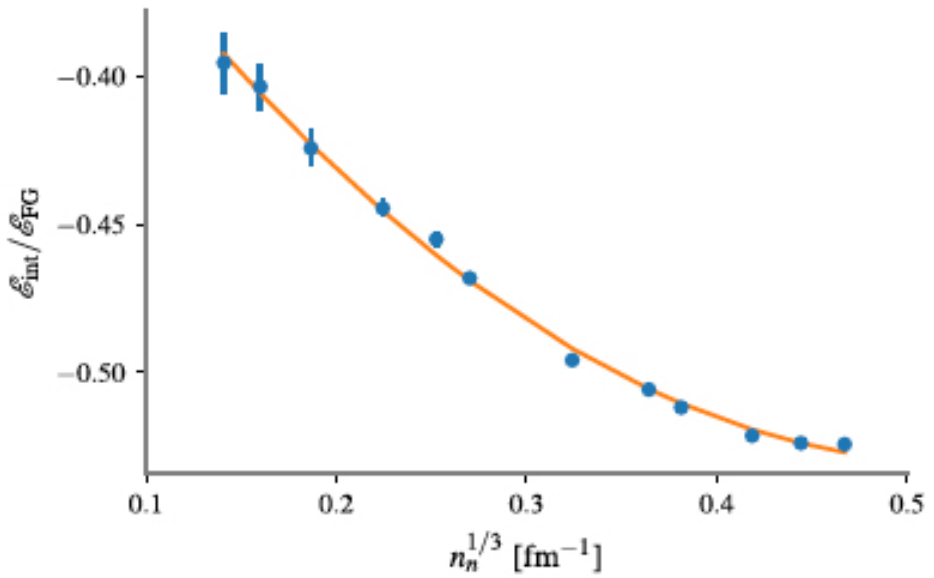

FIG. 3. The QMC results of Wlazłowski *et al.* [131] for the interaction energy per neutron displayed as the ratio $\mathcal{E}_{\rm int}/\mathcal{E}_{\rm FG}$ defined in Eq. (15b) (with $\beta = 1$), where $\mathcal{E}_{\rm FG} = 3\hbar^2(3\pi^2 n_n)^{2/3} n_n/(10m_n)$. If $a_n = 0$ in Eq. (15b), the ratio $\mathcal{E}_{\rm int}/\mathcal{E}_{\rm FG}$ would tend to 0 for $n_n \to 0$. For densities $n_n^{1/3}|a_{nn}| < 1$ (where $a_{nn} = -18.9$ fm is the s-wave neutron-neutron scattering length), the leading-order correction to the kinetic energy density per particle contribution would be instead linear in density $4\pi\hbar^2 a_{nn} n_n/m_n$.

The term proportional to $n^{5/3}$ is clearly present, as in the case of the unitary Fermi gas!

TABLE II. Best-fit parameters for the SeaLL1 functional and the orbital-free approximation (next column in italic when different). The errors quoted for the fit parameters should be interpreted as estimating by how much this parameter can be independently changed while refitting the other and incurring a cost of at most $\delta\chi_E < 0.1$ MeV.

	SSeaLL1	Hydro	Comments
n_0	0.154	*0.154*	Adjusted (see Fig. 5)
a_0	0	Same	Insignificant
b_0	−684.5(10)	*−685.6(2)*	
c_0	827.26	*828.76*	$2c_0 n_0^{\frac{2}{3}} = -\frac{3\hbar^2}{10m}(\frac{3\pi^2}{2})^{\frac{2}{3}} - \frac{3}{2}b_0 n_0^{\frac{1}{3}}$
a_1	64.3	*50.9*	$a_1 = n_0^{1/3} b_1$
b_1	119.9(61)	*94.9(14)*	
c_1	−256(25)	*−160.0*	Fixed in orbital-free theory
a_2	−96.8	*−83.5*	$a_2 = a_n - a_0 - a_1$
b_2	449.2	*475.2*	$b_2 = b_n - b_0 - b_1$
c_2	−461.7	*559.6*	$c_2 = c_n - c_0 - c_1$
a_n	−32.6	Same	From neutron matter EoS (16)
b_n	−115.4	Same	From neutron matter EoS (16)
c_n	109.1	Same	From neutron matter EoS (16)
η_s	3.93(15)	*3.370(50)*	
W_0	73.5(52)	*0.0*	Fixed in orbital-free theory
g_0	−200	N/A	g_0 fit in Ref. [145]
κ	N/A	*0.2*	Semiclassical (see Sec. III H)
$\frac{\hbar^2}{2m}$	20.7355	Same	Units (MeV = fm = 1)
e^2	1.43996	Same	cgs units ($4\pi\epsilon_0 = 1$)
χ_E	1.74	*3.04*	606 even-even nuclei
		2.86	2375 nuclei
χ_r	0.034	*0.038*	345 charge radii
		0.041	883 charge radii

- **In the orbital free framework there are four independent parameters:**

a_0, b_0, b_1, η_s.

- **Using single-particle orbitals there are seven independent parameters:**

a_0, b_0, b_1, c_1, W_0, η_s, and g_0.

These parameters are fixed by

- ✓ **Nuclear saturation density**
- ✓ **Binding energies of nuclei**
- ✓ **Symmetry energy and its density dependence**
- ✓ **Surface tension**
- ✓ **Spin-orbit strength**
- ✓ **Strength of pairing correlations**

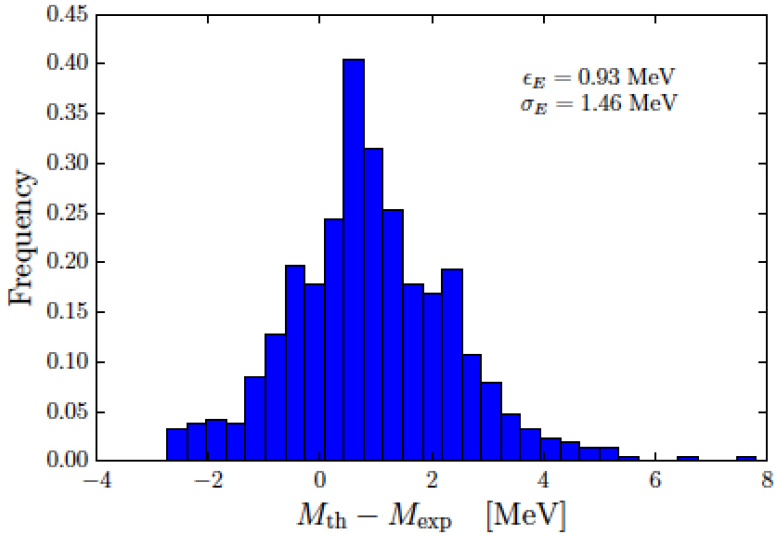

FIG. 9. The histogram of the mass residuals between SeaLL1 and experiment for 606 even-even nuclei.

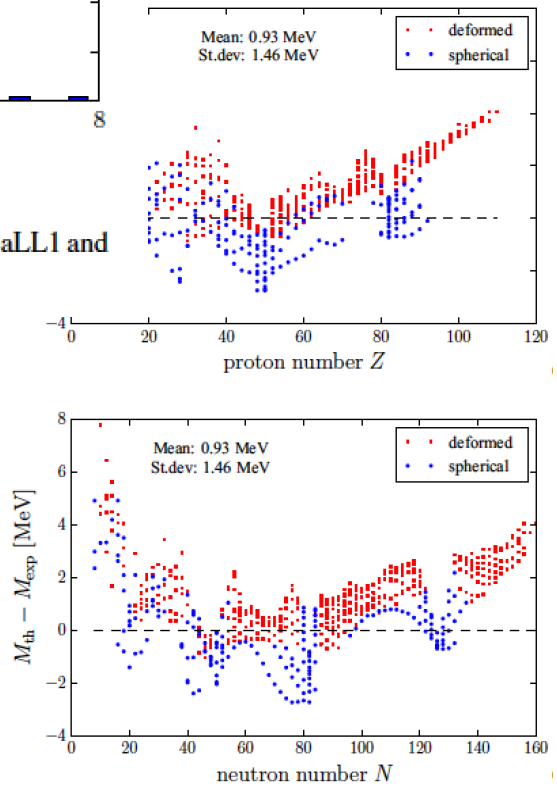

FIG. 8. Mass residuals between SeaLL1 and measured masses 606 even-even nuclei, of which 410 are deformed nuclei and 196 spherical nuclei, plotted with red squares and blue bullets respectiv as a function of proton number Z (a) and neutron number N (b).

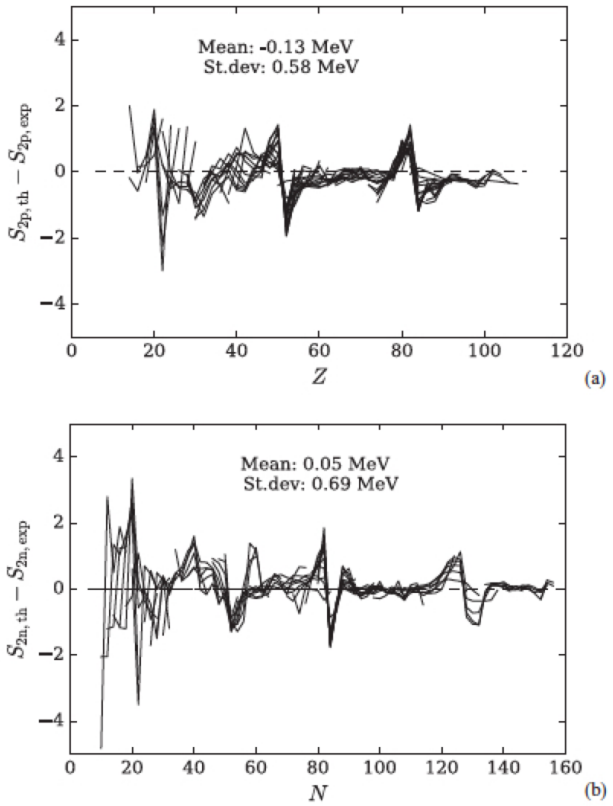

FIG. 10. The residual of the two-nucleon separation energies between SeaLL1 and experiment for 606 even-even nuclei: $S_{2p}(Z)$ for constant N (a) and $S_{2n}(N)$ for constant Z (b) chains connected by lines.

Introducing the center-of-mass correction for spherical nuclei alone reduce the χ_E for the binding energies from 1.54 MeV to 0.97 MeV. For spherical nuclei one needs also zero-point energy corrections.

Charge radii and charge distributions

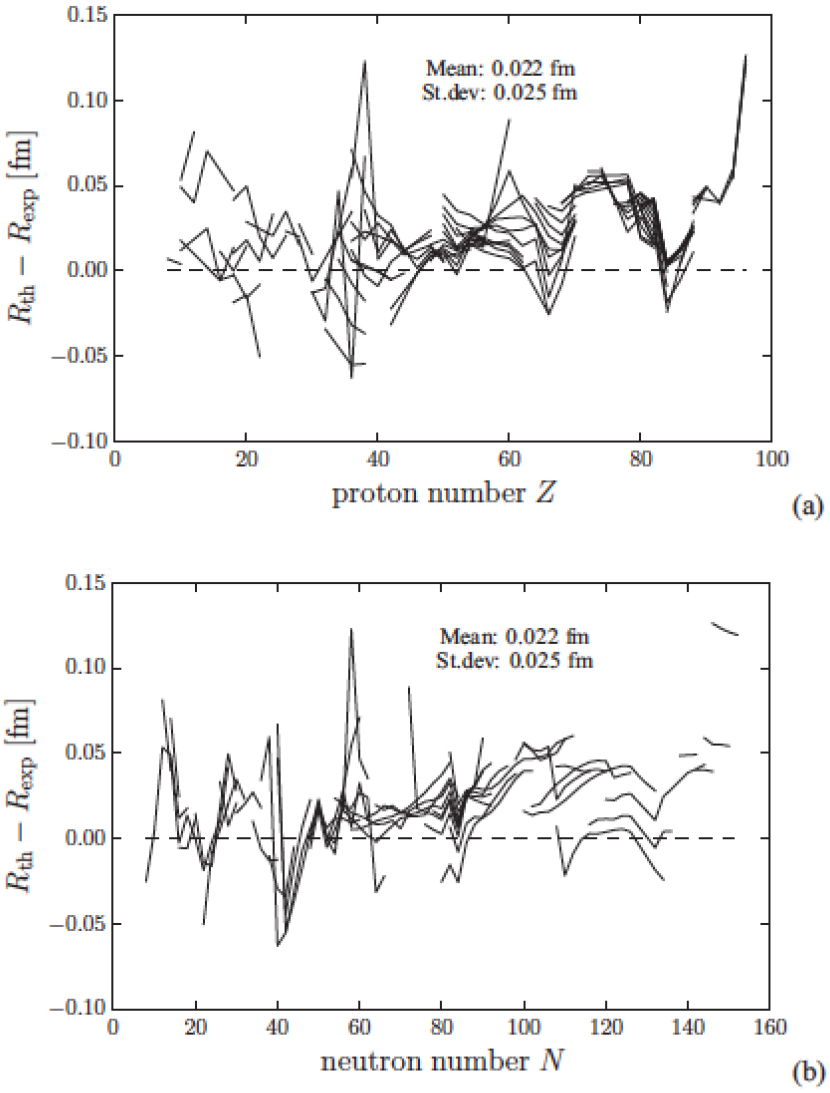

FIG. 12. Radii residuals between SeaLL1 and experiment for 345 even-even nuclei. Isotonic (a) and isotopic (b) chains are connected by lines.

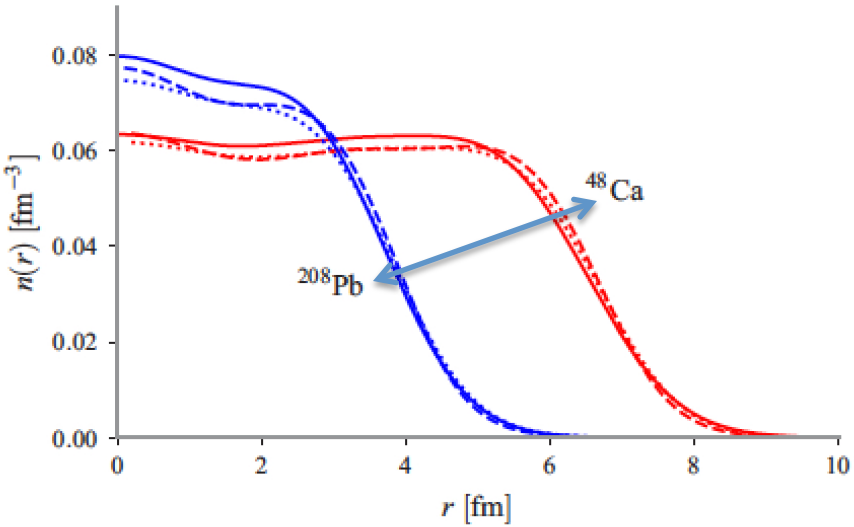

FIG. 11. The calculated proton $n_p(r)$ (dashed) and charge $n_{ch}(r)$ (dotted) densities for ^{48}Ca (red) and ^{208}Pb (blue), calculated with SeaLL1 compared to charge densities (solid) extracted from electron scattering experiments [157].

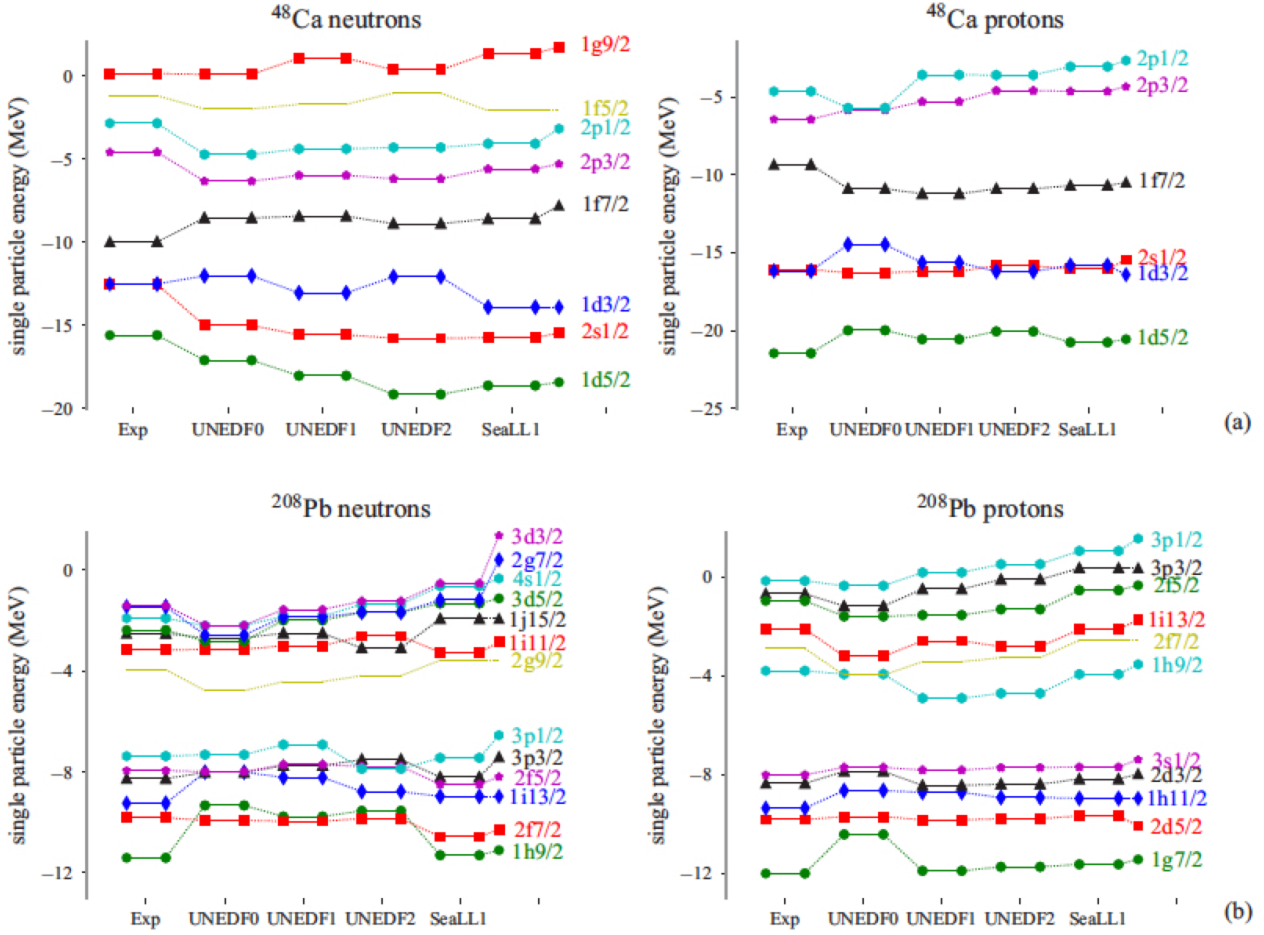

FIG. 13. Single particle energies in ^{48}Ca (a) and ^{208}Pb (b) for a variety of functionals UNEDF0-2 [73–75] and SeaLL1 (calculated using the HFBTHO DFT solver [154]).

^{48}Ca: rms deviations for UNEDF0, UNEDF1, UNEDF2, and SeaLL1 for neutrons/protons: 1.50/1.22, 1.71/1.08, 1.92/1.22, 1.88/1.17 MeV

^{208}Pb: rms deviations for UNEDF0, UNEDF1, UNEDF2, and SeaLL1 for neutrons/protons: 0.82/0.77, 0.61/0.49, 0.69/0.50, 0.62/0.54 MeV

UNEDF2 was constrained to describe single-particle properties too!